RESEARCH PAPER

DAILY VARIATIONS IN WET DEPOSITION AND WASHOUT RATES OF POTENTIALLY TOXIC ELEMENTS IN MOSCOW DURING SPRING SEASON

Dmitry V. Vlasov[1*], Irina D. Eremina[1], Galina L. Shinkareva[1], Natalia E. Chubarova[1], Nikolay S. Kasimov[1]
[1]Lomonosov Moscow State University, Leninskie gory 1, Moscow, 119991, Russian Federation
***Corresponding author:** vlasgeo@yandex.ru
Received: October 2th, 2020 / Accepted: February 16th, 2021 / Published: April 1st, 2021
https://DOI-10.24057/2071-9388-2020-162

ABSTRACT. For the first time, the wet deposition and washout rates of soluble forms of potentially toxic elements (PTEs) were estimated in rains during the spring AeroRadCity experiment in Moscow. Rains are an important factor in reducing atmospheric pollution with PTEs in Moscow. Due to the resuspension of contaminated particles of road dust and urban soils, industrial and traffic impact, waste and biomass burning, rainwater is highly enriched in Sb, Pb, Se, Cd, and S, and less enriched in P, Ba, As, W, Mn, Sn, Na, Co, Ni, and Be. Significant wet deposition (μg/m^2 per event) and washout rates (μg/m^2 per hour) of PTEs were revealed during the public holidays in May which corresponded to the elevated aerosol content due to predominant air advection from southern and south-western regions in this period. During continuous rains, the level of PTEs wet deposition sharply decreases on the second and subsequent days due to the active below-cloud washout of aerosols during the initial precipitation events. We show that the length of the dry period and aerosol content before the onset of rain determines the amount of solid particles in rainwater, which leads to an increase in rainwater pH, and strongly affects wet deposition and washout rates of PTEs of mainly anthropogenic origin (W, Zn, Bi, Cd, Sb, Ni, B, S, K, and Cu). At the same time rainfall intensity contributes to an increase in wet deposition and washout rates of Se, As, B, Cu, Sb, S, Cd, Ba, Rb, and K. The obtained results provide a better understanding of atmospheric deposition processes and can be useful in assessing the urban environmental quality.

KEY WORDS: wet deposition; washout rate, urban environment; contamination of precipitation; soluble forms of chemical elements

CITATION: Dmitry V. Vlasov, Irina D. Eremina, Galina L. Shinkareva, Natalia E. Chubarova, Nikolay S. Kasimov (2021). Daily Variations In Wet Deposition And Washout Rates Of Potentially Toxic Elements In Moscow During Spring Season. Geography, Environment, Sustainability, Vol.14, No 1, p. 219-233 https://DOI-10.24057/2071-9388-2020-162

ACKNOWLEDGEMENTS: Field and laboratory works as well as study of wet deposition rates of potentially toxic elements (PTEs) and source identification of PTEs in rainwater were done with the financial support of the Russian Science Foundation (grant number 19–77–30004). Assessment of the washout rates of PTEs from the atmosphere by rains has been supported by the Interdisciplinary Scientific and Educational School of M.V. Lomonosov Moscow State University «Future Planet and Global Environmental Change». The authors are grateful to E.V. Volpert for preparing data on the duration of precipitation.

Conflict of interests: The authors reported no potential conflict of interest.

INTRODUCTION

The study of the chemical composition of atmospheric precipitation makes it possible to assess the washout rates of potentially toxic elements (PTEs), particulate matter, organic pollutants and ions (such as sulfates, nitrates, ammonium, etc.) from the atmosphere and to evaluate wet deposition fluxes on the Earth's surface (Al-Momani 2008; Cizmecioglu and Muezzinoglu 2008; Bayramoğlu Karşı et al. 2018; Talovskaya et al. 2018, 2019; Ma et al. 2019; Tian et al. 2020; Cherednichenko et al. 2020; Park et al. 2020; Loya-González et al. 2020; McHale et al. 2021). PTEs usually include a large number of elements, e.g. carcinogenic As, Cd, Pb, Cr, Be, Ni, and Co, as well as causing general toxic damage to the body or individual organs and systems Sb, Zn, Cu, Mo, W, Sn, Se, Ba, Mn, and others (R 2.1.10.1920-04 2004; U.S. EPA 2020). Atmospheric precipitation is the most important factor in the self-purification of atmospheric air during the warm season (Ouyang et al. 2019; Long et al. 2020; Orlović-Leko et al. 2020). Wet deposition compared to dry one is more efficient in removing PTEs from the atmosphere and causes higher pollutants input into terrestrial or aquatic systems (Ouyang et al. 2015). Although estimates of wet deposition of PTEs over long periods of time (one-year or long-term) are carried out quite often, short-term changes in the chemical composition of rainwater are still poorly investigated (Pan et al. 2017).

The elemental composition of atmospheric precipitation has been studied in detail in many cities around the world. In Russia, the main attention is paid to the analysis of the individual chemical elements distribution in the rains, but those are usually snap-shot observations (Elpat'evskii 1993; Golubeva et al. 2005; Chudaeva et al. 2008; Udachin et al. 2010; Yanchenko and Yaskina 2014; Semenets et al. 2017; Svistov et al. 2017; Kuderina et al. 2018; Bufetova 2019). In Moscow – the largest megacity in Europe – complex meteorological observations are being carried out since the mid-1950s (Chubarova et al. 2014)

at the Meteorological Observatory of the Lomonosov Moscow State University (MO MSU). Since 1982, these observations have been supplemented with monitoring of the physicochemical properties and macrocomponent composition of atmospheric precipitation (Eremina 2019). The atmospheric air pollution in Moscow with particulate matter (PM) and gaseous pollutants, especially sulfur dioxide due to the use of natural gas by electric and thermal power plants, is lower than in other megacities (Elansky et al. 2018). In Moscow, research on the individual rain samples pollution with organic compounds was carried out (Polyakova et al. 2018). Our previous study of the solubility and partitioning of PTEs during spring rains in Moscow showed that anthropogenic sources contributed significantly to the concentration of soluble PTEs; for the insoluble PTEs, crustal materials were the important contributors (Vlasov et al. 2021a). The spring period was chosen because of the largest variety of meteorological conditions, typical for both cold and warm seasons, and emissions of pollutants into the atmosphere from various sources that were previously observed during spring months (Chubarova et al. 2019; Elansky et al. 2020; Popovicheva et al. 2020a). However, studies of the intensity of soluble PTEs washout from the atmosphere by rains within the city have not been previously conducted. Therefore, the aims of this study are to estimate wet deposition of soluble PTEs forms and to identify the rain parameters that affect PTEs washout from the atmosphere during the spring period.

MATERIALS AND METHODS

The study of the rainwater chemical composition was carried out in April-May 2018 at the MO MSU during the AeroRadCity experiment (Chubarova et al., 2019). The MO MSU is located in the southwestern part of the city at the territory of the MSU Botanical Garden, far from industrial sources of pollution and major highways; and therefore is considered as a background city station (Fig. 1). Rain samples (n = 15) were taken at a height of 2 m from the ground surface using a vinyl plastic funnel 80x80 cm in size and a white plastic bucket. Each rainfall event was analyzed from its beginning to the end on the current or adjacent days, that is, individual rainfall events: on April 6–7, 10–11, 17–18, 18–19, 21, 21–22, 25, 26, and May 1, 2, 4, 5–6, 17–18, 18–19, 19–20.

The pH and electrical conductivity (EC, μS/cm) were measured in rainwater samples by potentiometric and conductometric methods, respectively. To isolate soluble forms of PTEs, samples were filtered through Millipore© filters with a pore diameter of 0.45 μm. According to the mass of suspension on the filter, the content of solid particles in rainwater (*S*, mg/L) was estimated as $S = m / V$, where m is the mass of particles on the filter, mg; V is the volume of filtered rainwater, L. Concentrations of Al, As, B, Ba, Be, Bi, Ca, Cd, Co, Cr, Cu, Fe, K, Mn, Mo, Na, Ni, P, Pb, Rb, S, Sb, Se, Sn, W, and Zn in the filtrate were determined using mass spectral (ICP-MS) and atomic emission methods (ICP-AES) with inductively coupled plasma on the mass spectrometer «iCAP Qc» (Thermo Scientific, USA) and atomic emission spectrometer «Optima-4300 DV» (Perkin Elmer, USA) in the laboratory of the

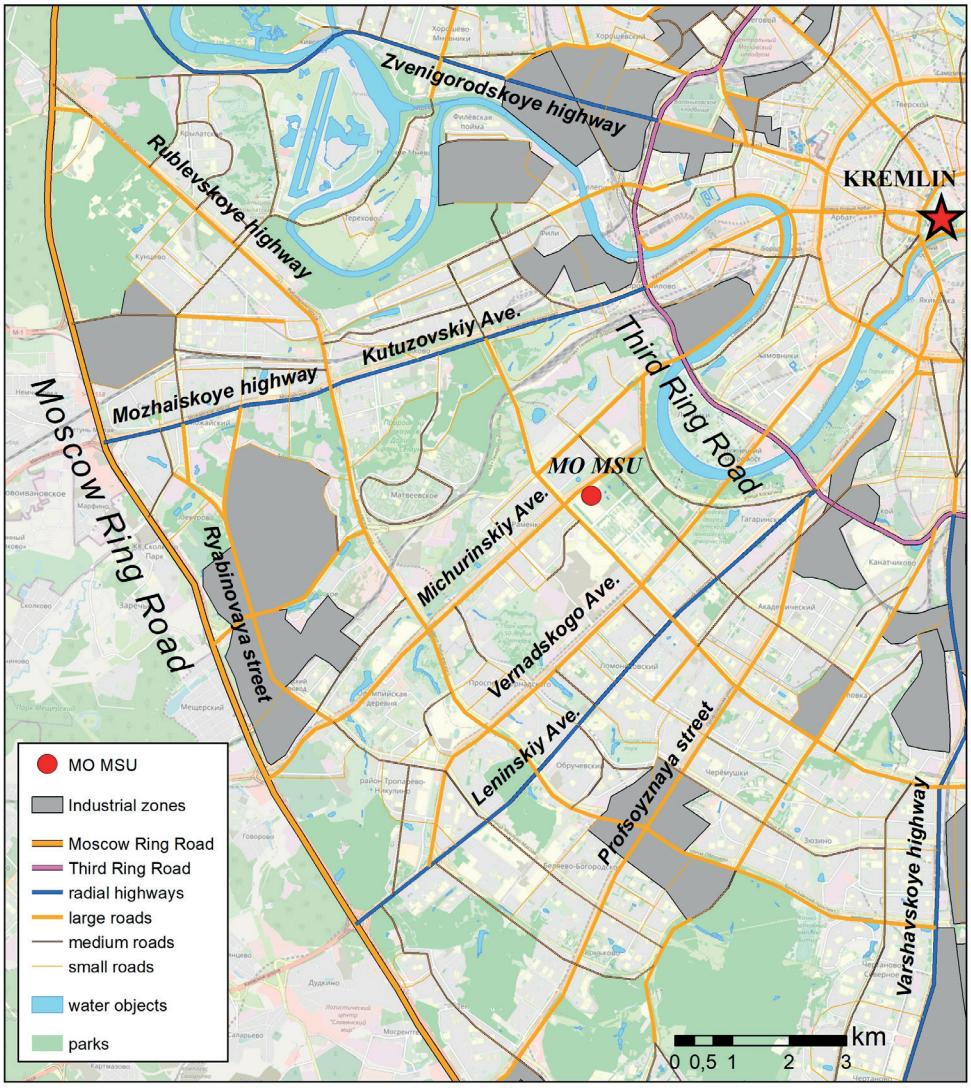

Fig. 1. Rains sampling site (MO MSU) in the southwestern part of Moscow

All-Russian Scientific-research Institute of Mineral Resources named after N.M. Fedorovsky according to certified methods (NSAM № 520 2017).

In this study, the term *wet deposition (D)* means the mass of a chemical element fallout from the atmosphere with rainfall per unit area of the Earth's surface for the entire precipitation event (μg/m^2 per event): $D = C \cdot X$, where C is the PTEs content in rainwater, μg/L; X is the precipitation amount, mm (which corresponds to L/m^2). The term *washout rate (Dh)* means the mass of a chemical element fallout from the atmosphere with rainfall per unit area of the Earth's surface per unit time (μg/m^2 per hour). The washout rate shows how effectively (quickly) the pollutant is washed out from the atmosphere: $Dh = C \cdot X / t$, where t is the duration of precipitation, hours. The Dh index allows to compare precipitation events of various duration to determine the effect of rainfall parameters on the intensity of PTEs washout from the atmosphere. The duration of precipitation was calculated as a difference between the end and the beginning times of a particular precipitation event. These data were obtained from the standard meteorological TM-1 tables and have an error in determining the beginning and the end of the precipitation event on the order of 1–2 minutes, which is more accurate than the 10-minute time resolution of measurements obtained with the pluviograph. At the same time, good correspondence was observed between the data on the duration of precipitation and the pluviograph data. The precipitation intensity (U, L/m^2 per hour) was also estimated as $U = X / t$. From the time difference between the end of the precipitation event and the beginning of the next one, the length (in hours) of the dry period R between rain events was calculated.

Due to big variation in wet deposition between particular PTEs, for a comprehensive assessment of each separate precipitation event, all data were normalized: $D'_i = (D_i - D_{min}) / (D_{max} - D_{min})$, where D_i and D'_i are the initial and normalized values of PTEs wet deposition in the i-th precipitation event, respectively; D_{max} and D_{min} are the maximum and minimum values of PTEs wet deposition for the entire observation period. Then the total normalized wet deposition (ND) in the i-th precipitation event can be defined as $\Sigma D'_{ij}$, where j are all considered PTEs (in our case, $j = 1, 2, 3, \ldots, 24, 25, 26$). The normalization was done for the wet deposition of PTEs to the Earth's surface (ND), as well as for data on the washout rate of PTEs from the atmosphere (NDh).

Statistical processing of the results was performed in the Statistica® 8 software. To assess the correlation between precipitation parameters (X, t, U, R) and the physicochemical properties of rainwater (pH, EC, S) on one hand, and values of PTEs wet deposition (D) and the washout rates of PTEs from the atmosphere (Dh) on the other hand, the nonparametric Spearman's rank correlation coefficients r_s were calculated, the significance of which was tested at a level of $p < 0.05$. To determine the PTEs groups with a similar distribution of wet deposition, cluster analysis was performed using the PTEs grouping by the Ward's method with the similarity measure d = 1 – Pearson's r.

RESULTS AND DISCUSSION

Rain parameters and physicochemical properties of rainwater.

To characterize weather conditions and identify periods with typical synoptic situations in April–May 2018, meteorological data from the MO MSU and a synoptic maps archive were used (Weather maps… 2020). An analysis of the atmospheric circulation features showed that in early and mid-April, during the period of rainfall, the cyclonic type of circulation prevailed with air advection from the western and northern regions. On April 25–26, a low-gradient baric field was observed with a predominance of air advection from the northern regions. In the first decade of May, air masses from the south and southwest prevailed, and from May 17 to May 20, air advection from the west with a cyclonic type of circulation was observed.

In 2018, the average monthly air temperature values were 2–3°C higher than the corresponding values for 1954 to 2013 and amounted to 8.4°C in April and 16.7°C in May, which matches with the general trend of climate warming (Chubarova et al. 2014). The amount of precipitation fell within the normal range: in April it was 38 mm compared to 41 mm, in May – 50 mm compared to 55 mm according to the long-term measurements. The duration of precipitation varied from short-term rains (less than 4 hours) on April 6–7 and 21, May 2, 4 and 5–6 to 17 hours on May 18–19, and even 25 hours on April 17–18, thus, the rain intensity varied from 0.2 L/m^2 per hour to 2.9 L/m^2 per hour depending on the event (Fig. 2). With an increase in the

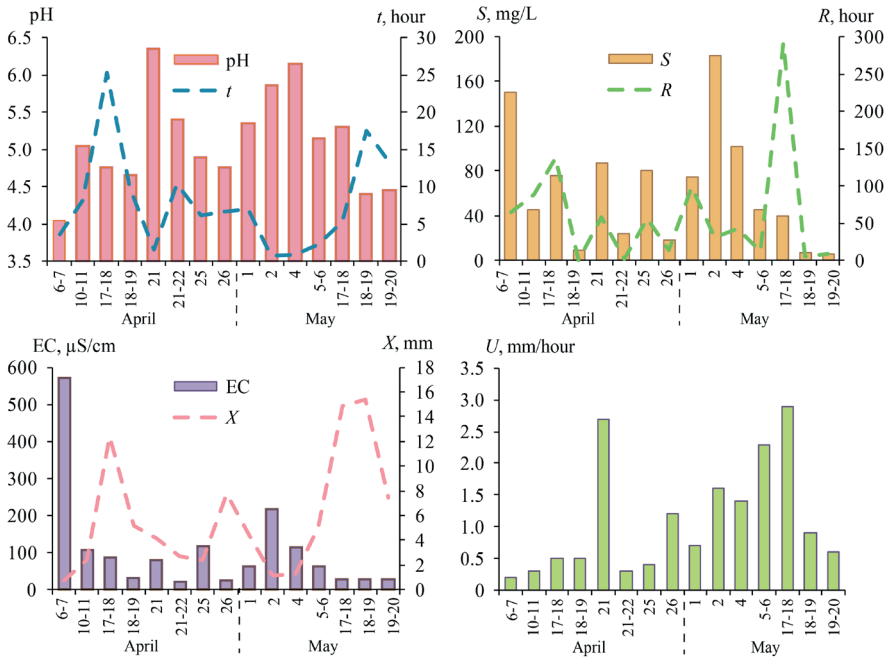

Fig. 2. Physicochemical properties of rainwater and rainfall parameters during the spring experiment. *X* – precipitation amount, *t* – duration of precipitation, *R* – length of the antecedent dry period, *S* – solid particles content in rainwater, *U* – precipitation intensity, EC – electrical conductivity

rain events duration, the precipitation amount also increases (r_s = 0.60; Fig. 3a), whilst the content of solid particles in rainwater decreases (r_s = 0.60; Fig. 3b) due to their intensive washout from the atmosphere at the beginning of precipitation event. As the duration of precipitation increases, the precipitation intensity usually decreases (Fig. 3c).

An excess of the acid precipitation (with pH < 5.0) frequency in April in comparison with the mean values for 35 years at the MO MSU (66% and 17%, respectively) was revealed. At the same time, a lower acid precipitation frequency was found for May (28% and 35%, respectively). All rains were characterized by a slightly acidic to almost neutral reaction with pH variability from 4.05 on April 6–7 to 6.35 on April 21 (Fig. 2). The average pH of rainwater in April and May 2018 was 4.7 (versus the average long-term values for these months of about 5.0 and 4.8, respectively). The highest EC value (572 μS/cm) was also found on April 6–7. In rainwater samples from other days the EC varied from 21 μS/cm to 217 μS/cm (Fig. 2). During the spring experiment, as in the last 13 years, Ca^{2+} was the predominant cation, and Cl^- was the predominant anion in precipitation (Eremina 2019; Eremina and Vasil'chuk 2019). The increase in EC values in rainfall is probably due to the partial dissolution of particulate matter washed out from the atmosphere, as indicated by the strong rank correlation (r_s = 0.85) between EC and the content of solid particles in rainwater (Fig. 3e). The ranking is based on the increase in the values of rainwater properties and precipitation parameters – high ranks correspond to high values of indicators.

The average solid particles content in rainwater during the spring experiment was 63 mg/L, varying from 6.1 mg/L in the last episode of prolonged precipitation in late May to 183 mg/L on May 2 during the public holidays (1–9 May) celebrated in Russia (Fig. 2) which were also characterized by elevated aerosol loading due to predominant air advection from the south and south-western regions (Chubarova et al. 2020). The amount of solid particles washed out with rains depends on the length of the antecedent dry period prior to precipitation event (r_s = 0.53; Fig. 3f), which is associated with the accumulation of coarse aerosol particles in the air during a long dry period and their subsequent washout with precipitation. A significant correlation between the solid particles content in rainwater and precipitation amount (r_s = –0.75; Fig. 3g) was revealed. This is likely due to the dilution effect, namely the mineralization and the content of solid particles in rainwater decrease with increasing precipitation amount (Park et al. 2015). A decrease in EC with an increase in the precipitation amount (r_s = –0.72) is associated with the same phenomenon (Fig. 3h). The decrease in solid particles content in rainwater is influenced by an increase in the duration of precipitation (r_s = –0.70), probably due to the more intensive washout rate of solid particles in the first minutes and hours after the beginning of a rainfall event (Fig. 3b). A decrease in the solid particles content in rainwater with increasing duration of precipitation leads to a decrease in rainwater pH (Fig. 3d) since high pH is associated with the partial dissolution of particulate matter (Singh et al., 2016).

Thus, the most important rain parameters for wet deposition are precipitation amount, duration and intensity as well as the length of the dry period. All of them affect the pH and EC values along with the content of solid particles in rainwater.

Wet deposition and washout rates of PTEs from the atmosphere.

The wet deposition of PTEs in spring varies greatly – on average from 21884 μg/m² per episode for Ca to 0.12 μg/m² per episode for Be (Table 1).

The highest levels of wet deposition (> 100 μg/m² per event) are typical for Ca > S > Na > K > Pb > Fe > Al > Zn > P, while highest washout rates from the atmosphere (> 50 μg/m² per hour) are common for Ca > S > K > Na > Fe > Al > Pb > Zn. For other PTEs, the wet deposition as well as washout rates are much lower and decrease (Table 1). Ca, S, Na, and K are macroelements of atmospheric precipitation and natural waters; the presence of macroelements of the continental crust (Al and Fe) in high concentrations relative to other PTEs in rainwater is associated with crustal and terrigenious sources input; high washout rates of Zn, Pb, Mn, Ba, and Cu are caused by the industrial and vehicular impact, which is typical for most large cities (Galloway et al. 1982; Song and Gao 2009; Kamani et al. 2014; Vlastos et al. 2019).

A comprehensive assessment of the temporal heterogeneity of wet deposition and washout rates of PTEs from the atmosphere was carried out by calculating

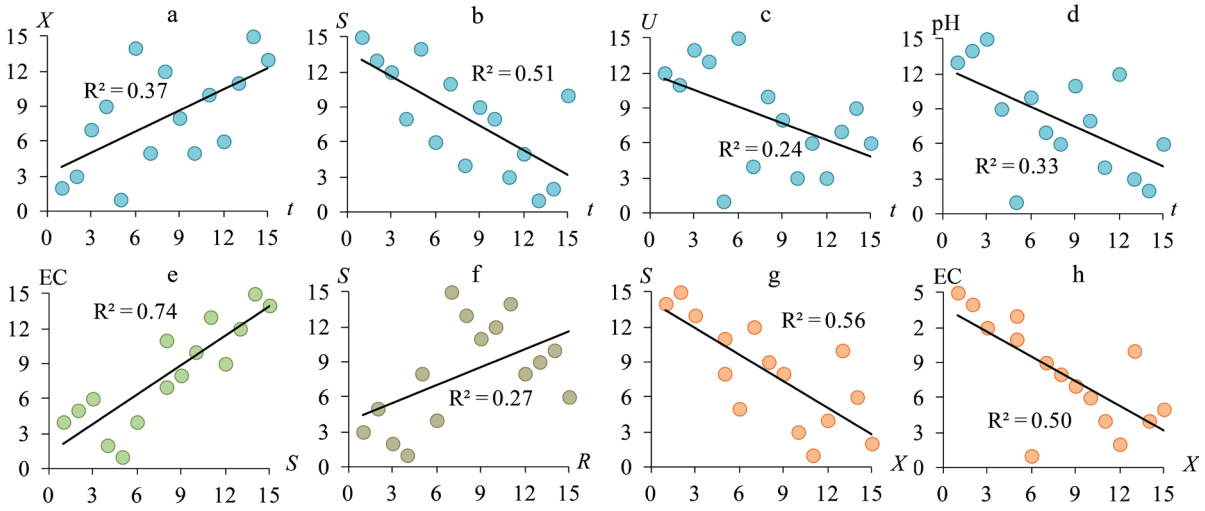

Fig. 3. Rank correlation between the ranks of the physicochemical properties of rainwater and rain parameters: *X* – precipitation amount, *t* – duration of precipitation, *R* – length of the antecedent dry period, *S* – solid particles content in rainwater, *U* – precipitation intensity, EC – electrical conductivity. High ranks correspond to high values of indicators. The color indicates the dependences on the same parameters of rain or the properties of rainwater (horizontal axis): (a)-(d) duration of precipitation, (e) solid particles content in rainwater, (f) length of the antecedent dry period, (g)-(h) precipitation amount

Table 1. PTEs' wet deposition to the Earth's surface and washout rates from the atmosphere at the MO MSU territory

PTEs	Wet deposition, μg/m² per event		Washout rates, μg/m² per hour	
	mean	minimum–maximum	mean	minimum–maximum
Ca	21884	3546–85152	6881	344–31420
S	3519	660–12279	991	64–3496
Na	1979	466–9113	497	35–1608
K	1269	173–3691	546	10–3828
Pb	650	38–3186	79	6.0–190
Fe	592	104–2615	111	10–238
Al	406	39–1860	96	3.8–300
Zn	214	42–922	58	4.0–247
P	123	16–481	42	0.92–278
Ba	95	17–272	24	1.6–82
Mn	76	15–264	28	1.1–165
Cu	51	10–213	10	0.98–35
B	32	3.1–161	7.6	0.31–34
Sb	19	3.1–83	5.4	0.30–23
Ni	2.8	0.51–13	0.78	0.050–4.1
Rb	2.3	0.63–5.8	1.0	0.061–7.4
Cr	1.7	0.43–6.9	0.43	0.042–2.1
Co	1.2	0.20–5.9	0.35	0.020–1.6
Se	0.89	0.18–2.3	0.17	0.039–0.43
As	0.73	0.14–1.7	0.17	0.029–0.74
Mo	0.58	0.070–1.5	0.11	0.020–0.29
Cd	0.55	0.13–1.9	0.14	0.012–0.45
W	0.21	0.038–1.0	0.048	0.004–0.18
Sn	0.2	0.027–0.96	0.057	0.003–0.23
Bi	0.14	0.024–0.73	0.034	0.002–0.11
Be	0.12	0.009–0.53	0.018	0.001–0.058

Note. PTEs are arranged in descending order of their average wet deposition

the total normalized values of wet deposition (*ND*) and total normalized values of washout rates of PTEs (*NDh*) for the entire experiment period. Changes in the *ND* and *NDh* values are shown in Fig. 4.

The highest *ND* values for the majority of PTEs were found for rains on April 17–18, when one of the three rainfall events with the highest precipitation amount (12.4 mm) was observed. These maxima are also associated with the highest aerosol concentration before the beginning of rainfall: from April 11 to April 16, the maximum PM_{10} concentration was observed over the entire period of the experiment and was equal to 43 μg/m³ (Chubarova et

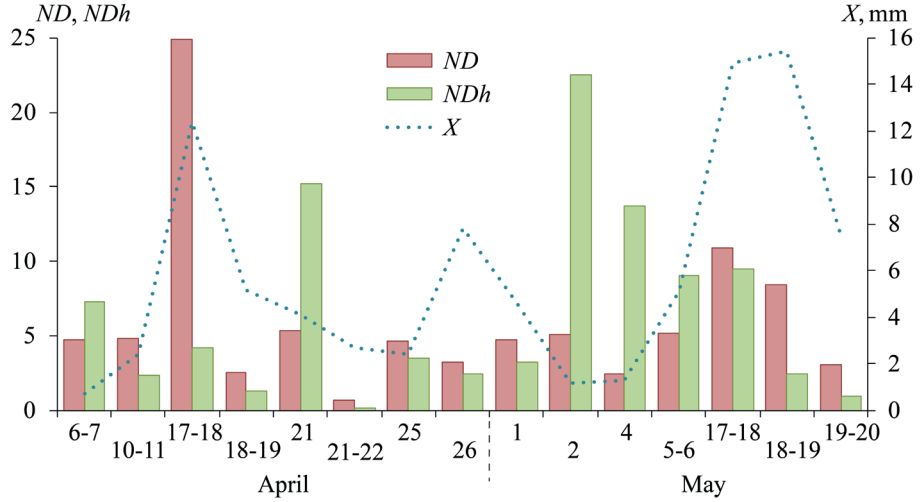

Fig. 4. Total normalized values of wet deposition of PTEs (*ND*, left axis) and washout rates of PTEs from the atmosphere (*NDh*, left axis), as well as precipitation amount (*X*, mm, right axis) on the MO MSU in April–May 2018

al. 2019). Afterwards, from April 17 to April 22, due to the precipitation and washing out of aerosols, a sharp decrease in the PM_{10} content (to 24 μg/m³) was determined, which in turn caused the high values of total normalized wet deposition on April 17–18 and total normalized washout rates on April 21. Increased levels of total normalized wet deposition of PTEs, relative to other days, were observed on May 17–19, which is also due to a high level of aerosol pollution of the atmospheric surface layer in the previous dry period (Chubarova et al. 2019), large precipitation amount (14.9–15.4 mm) and high rain intensity on May 17–18 (2.9 mm/hour, the most intense rain of the entire experiment period).

The washout rates of PTEs from the atmosphere have a slightly different pattern in temporal changes compared to *ND* (Fig. 4). Very high total normalized washout rates of PTEs (*NDh*) were revealed for May 1–6, when air advection from the south and southwest prevailed. The beginning of this period of public holidays (May 1) is characterized by rather low washout rates of PTEs. However, already on May 2 it increased sharply due to the anthropogenic emission of PTEs to the atmosphere from the biomass burning in suburban areas and the territory of the MSU Botanical Garden, together with the coal burning during picnics near MSU and vehicle emissions due to the large number of traffic jams that occur when residents leave the city. This is confirmed by the increase in the levels of wet deposition of K, Rb, Mn, Sn, Sb, and As these days, which are often used as indicators of controlled biomass and coal combustion or forest fires (Landing et al. 2010; Samsonov et al. 2012; Grivas et al. 2018). Thus, the spring period is characterized by a strong influence of forest fires in the Moscow region and the biomass burning in residential areas on the composition of atmospheric particles in Moscow (Popovicheva et al. 2020a), which is indicated by the high values of the black carbon (BC) to the PM_{10} content ratio in the atmosphere (Popovicheva et al. 2020b), since BC is a marker of biomass burning or fuel combustion.

From April 30 to May 5, a high concentration of PM_{10} of 34 μg/m³ was observed, which sharply decreased to 23 μg/m³ in the period from May 6 to May 12 (Chubarova et al. 2019), probably due to short and intense rains on May 2, May 4 and May 5–6, which caused high values of the total normalized washout rates of PTEs. On May 17–18, the PTEs washout rates were also high due to the previous long dry period (11 days), with a large amount of aerosol accumulated in the air on May 13–17, which resulted in high PM_{10} values (Chubarova et al. 2019). During prolonged rains, which lasted several days with only short breaks, wet deposition and PTEs washout rates significantly decreased, which is typical for May 18–19, May 19–20 and April 26, but especially noticeable for April 18–19 and April 21–22 (Fig. 4). These data confirm the hypothesis about the deposition of the main pollutants' masses in the first hours after the onset of rain due to the active washout of aerosols from the atmosphere (Lim et al. 1991).

Thus, the highest *ND* levels for most PTEs were found on April 17–18 and May 17–18 due to a long dry period before these precipitation events (138 hours and 292 hours, respectively) and high aerosol concentrations in the surface atmospheric layer. The maximum *NDh* was observed on April 21, May 2, May 4, May 5–6, and May 17–18 with relatively short and intense (1.4–2.9 mm/hour) precipitation.

Sources of PTEs in rainwater.

In order to estimate the contribution of anthropogenic sources to the content of PTEs in precipitation the enrichment factor (*EF*) could be used: $EF = (D_i/D_{Al})/(K_i/K_{Al})$, where D_i and D_{Al} are wet deposition of the *i*-th and the reference elements, K_i and K_{Al} are the abundances of the *i*-th and the reference elements in the upper continental crust (Rudnick and Gao 2014). Sometimes, when calculating *EF*, the average composition of seawater is used as a reference, and Na is applied as a reference element (Cheng et al. 2011); however, this approach overestimates *EF* values for typically crustal elements that have no significant anthropogenic sources (Si, Al, Ti, Zr, and others). Therefore, for the chemical composition of atmospheric precipitation studies, the content of PTEs in the upper continental crust is used as a reference standard with Al as a reference element (Basha et al. 2010). $EF < 10$ indicates a crustal (or terrigenous) origin of elements, *EF* from 10 to 100 shows probability of anthropogenic PTEs sources, and at $EF \geq 100$ PTEs definitely have an anthropogenic source (Tian et al. 2020).

High *EFs* in the Moscow rains in April–May 2018 certainly indicating the anthropogenic origin of the PTEs, were determined for (the *EF* values are shown in the subscript) Sb_{9392}, Pb_{7680}, Se_{1987}, Cd_{1232}, and S_{1138}. A significant contribution of anthropogenic sources was also observed for Zn_{641}, B_{373}, Cu_{368}, Bi_{175}, Ca_{171}, and Mo_{106}. In many other cities, a substantial enrichment of atmospheric precipitation with these PTEs was also found (Koulousaris et al. 2009; Song and Gao 2009; Özsoy and Örnektekin 2009; Landing et al. 2010; Kamani et al. 2014; Chon et al. 2015), and for Zn, Cd, and Cu it was reported even for the southeastern part of the Atlantic Ocean (Chance et al. 2015). This indicates the significant role of wet deposition processes for the PTEs input into terrestrial landscapes. The main sources of most of these PTEs are vehicle emissions, fuel combustion, tires and brake pads wear, road surface abrasion, roadside soil particles blowing, industrial enterprises emissions, as well as macroregional long-distance transport of pollutants (Demetriades and Birke 2015; Grigoratos and Martini 2015; Grivas et al. 2018; Konstantinova et al. 2020; Liyandeniya et al. 2020; Logiewa et al. 2020; Orlović-Leko et al. 2020; Ramírez et al. 2020; Seleznev et al. 2020; Tian et al. 2020), which is confirmed by the previously identified sources of snow cover pollution in the western part of Moscow (Vlasov et al. 2020). The remaining PTEs on the territory of the MO MSU were apparently of mixed anthropogenic-terrigenous sources (P_{38}, Ba_{31}, As_{30}, W_{22}, Mn_{20}, Sn_{19}, Na_{16}, Co_{14}, Ni_{12}, Be_{11}, K_{11}) and terrigenous origin (Rb_6, Cr_4, Fe_3), which indicates the influence of solid particles blown out from the Earth's surface and included in the atmospheric precipitation.

For a more detailed determination of PTEs sources, a cluster analysis was carried out. Based on its results, four associations of soluble forms of PTEs with similar deposition patterns were identified: (1) Zn–Sb–Ni–Ca–Co–Bi–Sn–Al–W–Cr–Fe–Na–P; (2) Cu–Ba–Pb–Cd–S–B; (3) Se–Mo–As–Be; and (4) K–Rb–Mn (Fig. 5).

The first geochemical association (Zn–Sb–Ni–Ca–Co–Bi–Sn–Al–W–Cr–Fe–Na–P) includes PTEs coming from anthropogenic (Zn, Sb, Bi, Ca), anthropogenic-terrigenous (W, Sn, Co, Ni, Na, P) and terrigenous (Al, Fe, Cr) sources. Sb, Zn, Sn, Bi, W, and Ni indicate the resuspension of road dust and its various grain size particles, since in Moscow and some other cities road dust is highly enriched with these PTEs (Ladonin and Plyaskina 2009; Fedotov et al. 2014; Ermolin et al. 2018; Kasimov et al. 2019a; Ladonin and Mikhaylova 2020; Vlasov et al. 2021b). For example, in the eastern part of Moscow, the fine fraction PM_1 and the coarser PM_{1-10} of road dust are significantly ($EF > 5$) enriched in Sb, W, Sn, Cd, Zn, Cu, Pb, Mo, and Bi, especially on Moscow Ring Road and highways (Vlasov et al. 2015; Kasimov et al. 2020). Al, Fe, and Na are emitted by blowing out particles of contaminated urban soils (Morera-Gómez et al. 2020). This source is somewhat less significant for W, which is presented in the surface horizons of Moscow soils (Kosheleva et al. 2018). Blown-out soil particles are also a source of P in atmospheric aerosols and precipitation (Bencharif-Madani et al. 2019). Deicing agents can supply Na and Ca, since $CaCl_2$ and marble chips $(Ca, Mg)CO_3$ are among the main deicing agents after NaCl in Moscow (Vlasov et al. 2020).

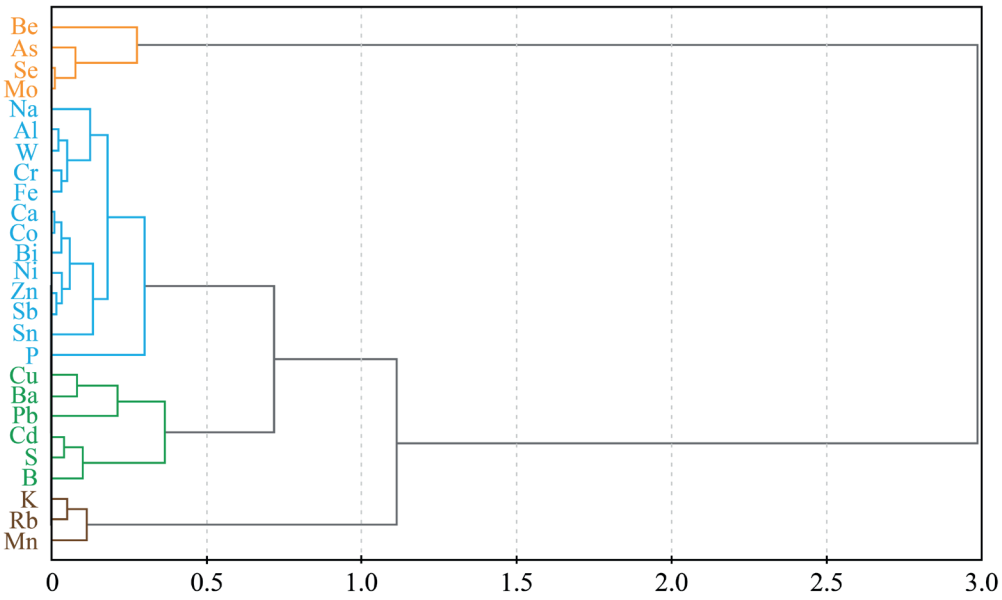

Fig. 5. Dendrogram of wet deposition of PTEs in the MO MSU on April–May 2018 (clustering was done using Ward's method; the similarity measure is *d* = 1 – Pearson's *r*)

Mentioned deicing agents are found in high concentrations in road dust and surface soil horizons in the spring season. Cr, Ni, and Co can come due to abrasion of the asphalt pavement (Song and Gao 2011). Thus, the Zn–Sb–Ni–Ca–Co–Bi–Sn–Al–W–Cr–Fe–Na–P association is mainly formed by the blown out particles of urban soils, road dust and deicing agents, which could be partially dissolved in rainwater. For instance, at the very beginning of the contact of an acidic (pH 4.7) mimicking fog water with atmospheric $PM_{2.5}$, a significant part of K, Cd, Mn, Mo, V, Ba, Al, Fe, Sb, Cu, and Cr are transferred to the soluble form (Di Marco et al. 2020).

The second association Cu–Ba–Pb–Cd–S–B includes elements with high *EFs*, that are coming from anthropogenic sources (Cu, Pb, Cd, S, B), as well as anthropogenic-terrigenous Ba. Copper, as well as Pb and Cd, are used in large quantities in vehicle brake pads and linings (Fabretti et al. 2009; Grigoratos and Martini 2015). Barium sulfates used in the brake pads manufacturing as a friction modifier can supply S and Ba to atmospheric particles and precipitation (Pant and Harrison 2013). Boron also comes from vehicles, since it is used as an additive in the manufacture of polymers, glass and fiberglass, as well as in the production of lubricants, antifreeze and fuel additives (U.S. Borax 2020). Waste incineration can be an additional source of Sb, Cd, and other PTEs (Christian et al. 2010). High S concentrations also often indicate a large contribution of long-distance transport of secondary inorganic aerosols (Cheng et al. 2015).

The third association (Se–Mo–As–Be) is formed by elements with very high (Se, Mo) and high (As, Be) *EFs*, which indicates their predominantly anthropogenic origin in atmospheric precipitation. Likely sources of Mo include metalworking, car repair and painting companies (Demetriades and Birke 2015; Zheng et al. 2018), widespread in Moscow. Arsenic, Se, Be and sometimes Mo can come from waste incineration and diesel fuel combustion (Kumar et al. 2015; Bencharif-Madani et al. 2019), while Se is also used as a coal combustion indicator (Wu et al. 2018). Despite the fact that coal is not used at Moscow thermal power plants, Se accumulated in fine particles (0.25–0.35 μm) could migrate hundreds of kilometers (Gallorini 2000) from those territories where coal is burned (suburbs, summer cottages, even transboundary transfer).

The fourth association (K–Rb–Mn) is probably determined by the biomass burning, since these PTEs, as noted above, are widely used as indicators of this type of impact (Samsonov et al. 2012; Grivas et al. 2018). High *EFs* values are found for Mn and K, while for Rb low *EF* is defined, probably due to its poor solubility in rainwater (Yu et al. 2018) and relatively high abundance in the upper continental crust.

Thus, the Zn–Sb–Ni–Ca–Co–Bi–Sn–Al–W–Cr–Fe–Na–P geochemical association is formed by the PTEs input mainly with blowing out of soil particles and road dust as well as deicing agents' resuspension. The main source of Cu–Ba–Pb–Cd–S–B association is vehicle emissions, while Se–Mo–As–Be association is particularly emitted from industrial sources as well as during waste incineration and long-distance air mass transport. In addition, biomass combustion (including forest fires) and atmospheric migration of plant pollen are responsible for the formation of K–Rb–Mn geochemical association.

Influence of rain parameters on the washout rates of PTEs from the atmosphere.

A nonparametric correlation analysis was carried out to determine the main factors affecting the wet deposition of PTEs to the Earth's surface and the PTEs washout rates from atmospheric air.

The precipitation amount determines the wet deposition values of anthropogenic PTEs with high *EFs* (Table 2, Fig. 6): Se, Mo (r_s = 0.96), As, Pb, Ba, and Cd (r_s 0.83, 0.65, 0.59, and 0.57, respectively). Other researchers also noted a similar positive correlation, for instance, in cities and suburbs of Northern China for Cu, Zn, Cd, As, and Se (Pan and Wang 2015), and Izmir, Turkey for Cr, Cd, Pb, and Ni (Cizmecioglu and Muezzinoglu 2008). Less strong inverse correlation was found between the precipitation amount and the washout rates of soluble PTEs from the atmosphere: r_s values are significant only for anthropogenic-terrigenous Na and P (–0.53); for other elements, except for Se, Mo, and Pb, they are also negative (Table 3, Fig. 7). A decrease in the PTEs washout rates is associated, as noted earlier, with the dilution effect, which reduces the PTEs concentrations and, as a consequence, the mass of pollutants' washout per unit time.

The duration of precipitation has a significant positive correlation with the wet deposition of PTEs of anthropogenic origin including Pb, Mo, Se, and As (r_s 0.63–0.53), and a negative correlation with the washout rate from the atmosphere for all PTEs (Tables 2 and 3, Figs. 6 and 7). Such relations are significant for all PTEs, except for Be and Pb, with r_s values ranging from –0.52 for Mo to –0.90 for Mn. The reason for this is a sharp decrease in PTEs concentrations in atmospheric air by the end of the precipitation event in comparison with its beginning, when

the highest PTEs levels are usually found, due to the removal of pollutants from the atmosphere during prolonged precipitation (Ouyang et al. 2015).

The length of the antecedent dry period is one of the most important factors contributing to an increase in wet deposition and the washout rates of PTEs from the atmosphere especially in conditions with elevated aerosol content (Tables 2 and 3, Figs. 6 and 7). This is most pronounced for the wet deposition of PTEs of anthropogenic (Bi, S, Zn, Cu, B, Ca), anthropogenic-terrigenous (Co, K, Mn, Na, Ni, W) and terrigenous (Al, Rb) origin. For the washout rates of most PTEs, such relations are less pronounced, while the correlation coefficients are positive for all PTEs and are significant for W, Ni, B, Be, Rb, and Cu (0.65–0.51). That is, with an increase in the dry period, the washout rate of PTEs increases.

The first rain after a long dry period is enriched with PTEs due to in-cloud and below-cloud scavenging processes. During a short dry period, due to frequent precipitation, the below-cloud scavenging processes weaken with the gradual removal of solid particles from the atmosphere (Bayramoğlu Karşı et al. 2018). During prolonged precipitation, an increased amount of aerosols is removed from the atmosphere within the first days. On the subsequent days, due to low concentrations of atmospheric aerosols, the rains wash out smaller amounts of pollutants. An increase in the pollutant concentrations in precipitation after a long dry period and a large load of contaminants in the early stages of river runoff are often referred to as the «first flush effect» that was investigated in detail on urban territories (Schiff et al. 2016; Shen et al. 2016; Liu et al. 2019; Mamoon et al. 2019).

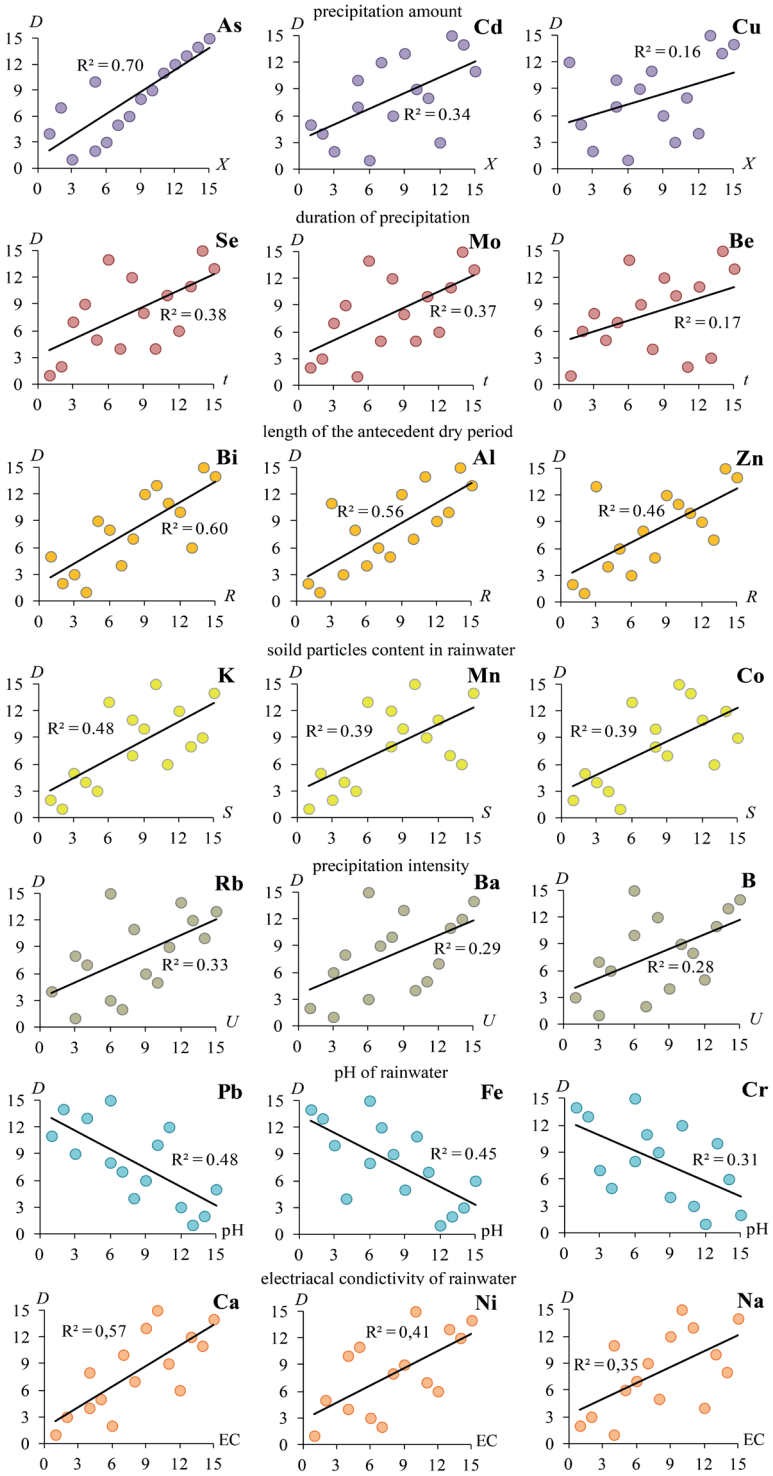

Fig. 6. Examples of rank correlation of wet deposition of PTEs (vertical axis) with the physicochemical properties of rainwater or rain parameters (horizontal axis; designations are shown in caption of Fig. 2). High ranks correspond to high values of indicators. The color shows the correlation with the same rain parameters or properties of rainwater

Table 2. The Spearman's correlation coefficient (r_s) values between wet deposition of PTEs on the Earth's surface, physicochemical properties of rainwater, and rain parameters on the MO MSU territory

PTEs	Physicochemical properties of rainwater			Rain parameters			
	pH	EC	Solid particles content	Precipitation amount	Duration of precipitation	Precipitation intensity	Length of the antecedent dry period
Be	–0.01	–0.17	–0.10	0.38	0.42	–0.11	0.47
B	0.29	–0.02	0.14	0.39	–0.13	**0.51**	**0.56**
Na	–0.07	**0.57**	**0.52**	–0.15	–0.16	–0.09	**0.66**
Al	–0.25	0.45	0.38	0.09	0.02	–0.06	**0.75**
K	0.46	0.46	**0.68**	–0.17	–0.49	0.39	**0.70**
P	0.10	0.31	0.36	–0.12	–0.21	0.08	0.25
S	0.06	0.27	0.28	0.21	–0.05	0.25	**0.72**
Ca	0.07	**0.74**	**0.74**	–0.31	–0.35	0.03	**0.68**
Cr	**–0.57**	0.36	0.15	0.15	0.17	–0.19	0.39
Mn	0.46	0.42	**0.61**	–0.05	–0.40	0.43	**0.69**
Fe	**–0.68**	0.15	–0.07	0.36	0.41	–0.27	0.47
Co	0.06	**0.62**	**0.63**	–0.15	–0.26	0.04	**0.79**
Ni	–0.18	**0.63**	**0.56**	–0.10	–0.08	–0.09	**0.63**
Cu	–0.39	0.18	0.06	0.39	0.28	–0.00	**0.60**
Zn	–0.10	0.38	0.33	0.19	0.01	0.14	**0.68**
As	–0.47	–0.47	**–0.60**	**0.83**	**0.53**	0.24	0.05
Se	–0.48	**–0.69**	**–0.72**	**0.96**	**0.60**	0.22	–0.05
Rb	0.45	0.36	**0.51**	0.06	–0.37	**0.55**	**0.65**
Mo	–0.35	**–0.72**	**–0.75**	**0.96**	**0.60**	0.31	–0.08
Cd	–0.18	–0.06	–0.18	**0.57**	0.24	0.30	0.35
Sn	0.06	**0.59**	0.48	–0.14	–0.11	0.00	0.48
Sb	0.00	0.27	0.18	0.29	0.01	0.30	0.49
Ba	0.06	–0.06	–0.06	0.59	0.14	**0.53**	0.44
W	–0.42	**0.52**	0.30	–0.03	0.19	–0.37	**0.64**
Pb	**–0.70**	–0.20	–0.40	**0.65**	**0.63**	–0.19	0.13
Bi	0.09	0.35	0.46	0.01	–0.24	0.12	**0.77**

Note. The r_s values significant at $p < 0.05$ are shown in **bold**

Table 3. The Spearman's correlation coefficients (r_s) values between washout rates of PTEs from the atmosphere, physicochemical properties of rainwater, and rain parameters on the MO MSU territory

PTEs	Physicochemical properties of rainwater			Rain parameters			
	pH	EC	Solid particles content	Precipitation amount	Duration of precipitation	Precipitation intensity	Length of the antecedent dry period
Be	0.43	0.28	0.48	–0.06	–0.50	**0.54**	**0.52**
B	**0.66**	0.28	**0.54**	–0.05	**–0.68**	**0.77**	**0.54**
Na	0.45	**0.69**	**0.82**	**–0.53**	**–0.81**	0.38	0.45
Al	0.43	**0.72**	**0.87**	–0.49	**–0.82**	0.42	0.50
P	0.45	**0.64**	**0.78**	**–0.53**	**–0.78**	0.34	0.31
S	**0.58**	**0.61**	**0.77**	–0.43	**–0.83**	**0.56**	0.48
K	**0.65**	**0.56**	**0.82**	–0.47	**–0.87**	**0.54**	0.50
Ca	0.50	**0.67**	**0.82**	–0.47	**–0.85**	**0.51**	0.47
Cr	0.34	**0.63**	**0.78**	–0.42	**–0.82**	0.45	0.46
Mn	**0.65**	**0.59**	**0.83**	–0.50	**–0.90**	**0.53**	0.47
Fe	0.30	**0.68**	**0.82**	–0.49	**–0.82**	0.38	0.48

Co	**0.51**	**0.68**	**0.84**	–0.49	**–0.87**	0.49	0.46
Ni	0.45	**0.69**	**0.86**	–0.46	**–0.80**	0.44	**0.55**
Cu	0.43	**0.52**	**0.70**	–0.23	**–0.71**	**0.61**	**0.51**
Zn	**0.51**	**0.66**	**0.83**	–0.43	**–0.83**	**0.53**	0.49
As	0.41	0.19	0.37	–0.13	**–0.77**	**0.78**	0.26
Se	0.34	0.01	0.21	0.13	**–0.67**	**0.90**	0.16
Rb	**0.63**	**0.57**	**0.76**	–0.43	**–0.85**	**0.59**	**0.51**
Mo	0.49	–0.19	0.03	0.31	**–0.52**	**0.96**	0.09
Cd	**0.54**	**0.63**	**0.80**	–0.43	**–0.84**	**0.54**	0.49
Sn	0.44	**0.76**	**0.81**	–0.50	**–0.66**	0.28	0.50
Sb	**0.53**	**0.62**	**0.78**	–0.35	**–0.76**	**0.56**	0.50
Ba	**0.53**	0.39	**0.57**	–0.07	**–0.65**	**0.76**	0.38
W	0.34	**0.74**	**0.85**	–0.46	**–0.68**	0.29	**0.65**
Pb	–0.38	0.11	0.09	0.35	–0.09	0.09	0.43
Bi	**0.56**	**0.61**	**0.83**	–0.48	**–0.85**	0.47	0.45

Note. The r_s values significant at $p < 0.05$ are shown in **bold**

Solid particles content in rainwater contributes to an increase in the wet deposition and washout rates of PTEs from the atmosphere due to the intensification of the gradual dissolution of particles, which in turn leads to an increase in the concentration of soluble forms of PTEs (Table 3, Fig. 7).

The rain intensity proved to have a positive correlation with the wet deposition of most PTEs. High significant r_s were found for terrigenous Rb (0.55), anthropogenic-terrigenous Ba (0.53), and anthropogenic B (0.51) (Table 2, Fig. 6). The washout rate is characterized by stronger correlation (Table 3, Fig. 7) with rain intensity for a large number of PTEs: high r_s values were found for Ca, Mn, Zn, Be, K, Cd, S, Sb, and Rb (0.51–0.59), Cu (0.61), Ba, B, As (0.76–0.78), and Se (0.90). For other PTEs, except for Pb, r_s is also positive and amounts to 0.37 and even higher. A positive correlation between the amount of PTEs washed out from the atmosphere and rain intensity is typical for precipitation in Kyoto and regions of Japan (Sakata et al. 2006), as well as for southwestern Taiwan, when during the typhoon, the amount of washed-out pollutants sharply increased compared to the usual precipitation levels (Cheng and You 2010).

Long dry periods before the onset of precipitation event lead to an increase in the solid particles' content in rainwater, which in turn contributes to an increase in the rainwater pH as a result of the partial dissolution of the suspended matter (Yeremina et al. 2014; Singh et al. 2016). Such partial dissolution of road dust particles can contribute to an increase in precipitation pH since its values for the water extract of road dust in Moscow is 6.4–8.1 (Kasimov et al. 2019b). Therefore, with an increase in the length of the dry period, as well as the amount of solid particles in rainwater and pH value, the intensity of PTEs washout by rain from the atmosphere also increases (Table 3, Fig. 7). The largest r_s values are typical for B, K, Mn, and Rb (r_s 0.66–0.63), as well as Co, Ba, Bi, Cd, Sb, S, and Zn (0.58–0.51). Due to the acidifying effect of industrial and thermal power plants emissions (e.g., on account of sulfate-ion formation as a result of a chemical reaction of emitted sulfur dioxide and water in the atmosphere), vehicle emissions (e.g., nitrate-ion formation as a result of chemical reactions of emitted nitrogen oxides and water), and also deicing chloride reagents (Eremina et al. 2015), a decrease in the rainwater pH is accompanied by an increase in the wet deposition of Pb (r_s = –0.70), Fe (–0.68), and Cr (–0.57), as well as Be, Na, Al, Ni, Cu, Zn, As, Se, Mo, Cd, and W (Table 2, Fig. 6). At the same time, a decrease in the rainwater pH in this case is not the reason for the growth of wet deposition of PTEs, but an indicator of the anthropogenic sources' impact on supplying these PTEs to the urban environment.

Electrical conductivity indirectly shows the amount of ions in the solution (rainwater). Therefore, EC has positive a correlation with the level of wet deposition of many PTEs, and especially Ca, Ni, Co, Sn, Na, and W (r_s 0.74–0.52). For some PTEs, this correlation is negative. This is possible because, due to the predominantly low levels of deposition of these PTEs (first of all, Be, Se, As, Mo, Cd, and Ba), their contribution to EC is insignificant. Therefore, the pattern of EC change is determined precisely by the behavior of elements with high concentrations in rainwater and, accordingly, high levels of wet deposition, e.g. Ca, Na, Fe, Mn, Al, S, etc. (Tables 2 and 3, Figs. 6 and 7). This is confirmed by the fact that positive significant r_s values were found between the washout rates of the majority of PTEs and the EC value.

CONCLUSIONS

In urban conditions, rain is an important factor in the atmosphere purification from PTEs. The contaminated particles of road dust and urban soils input into the atmosphere during wind-blowing, the impact of transport and industrial facilities, waste incineration and biomass burning lead to a strong enrichment of rainwater with soluble forms of Sb, Pb, Se, Cd, and S, as well as P, Ba, As, W, Mn, Sn, Na, Co, Ni, and Be. High levels of PTEs wet deposition were revealed for the public holidays (May 1–6), which is due to the anthropogenic supply of PTEs to the atmosphere during the combustion of organic residues and coal in suburbs, the strong impact of transport and the elevated aerosol content due to predominant air advection from southern and south-western regions. During prolonged rains, the wet deposition of PTEs sharply decreases on the second and subsequent days due to the active below-cloud scavenging of aerosols during the initial moments of precipitation.

In Moscow, one of the most significant rainfall parameters affecting the level of PTEs wet deposition from the atmosphere is the length of the dry period before the

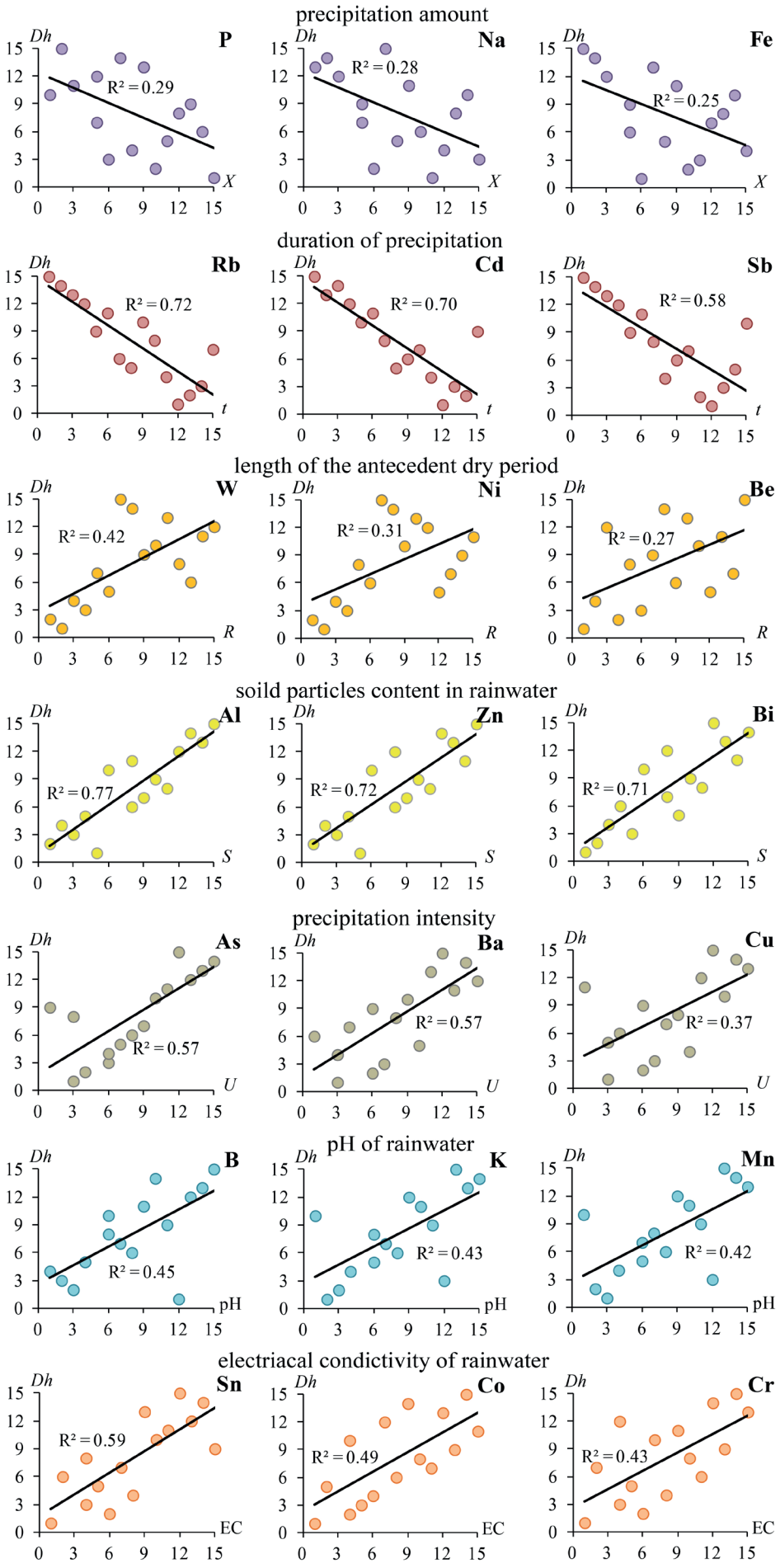

Fig. 7. Examples of rank correlation of washout rates of PTEs (vertical axis) with the physicochemical properties of rainwater or rain parameters (horizontal axis; designations are shown in caption of Fig. 2). High ranks correspond to high values of indicators. The color shows the dependences on the same rain parameters or properties of rainwater

beginning of atmospheric precipitation when aerosol particles accumulate in the air, which leads to an increase in rainwater pH. This factor has a particularly strong effect on the deposition and washout of PTEs of mainly anthropogenic origin (W, Zn, Bi, Cd, Sb, Ni, B, S, K, and Cu). Another important factor in atmosphere purification from PTEs is the rain intensity, which depends on the amount and duration of precipitation. An increase in these parameters leads to an increase in wet deposition and washout rates of most PTEs, especially of anthropogenic Se, As, B, Cu, Sb, S, and Cd, anthropogenic-terrigenous Ba and K, and terrigenous Rb.

The first data obtained for Moscow on the rain parameters affecting the levels of wet deposition and washout rates of PTEs from the atmosphere in April–May are preliminary. However, these results can be useful for urban environmental quality assessment in Moscow and can provide a better understanding of atmospheric deposition processes in urban areas.

REFERENCES

Al-Momani I. (2008). Wet and dry deposition fluxes of inorganic chemical species at a rural site in Northern Jordan. Archives of Environmental Contamination and Toxicology, 55(4), 558-565, DOI: 10.1007/s00244-008-9148-z.

Basha S., Jhala J., Thorat R., Goel S., Trivedi R., Shah K., Menon G., Gaur P., Mody K. and Jha B. (2010). Assessment of heavy metal content in suspended particulate matter of coastal industrial town, Mithapur, Gujarat, India. Atmospheric Research. 97(1-2), 257-265, DOI: 10.1016/j.atmosres.2010.04.012.

Bayramoğlu Karşı M., Yenisoy-Karakaş S. and Karakaş D. (2018). Investigation of washout and rainout processes in sequential rain samples. Atmospheric Environment. 190, 53-64, DOI: 10.1016/j.atmosenv.2018.07.018.

Bencharif-Madani F., Ali-Khodja H., Kemmouche A., Terrouche A., Lokorai K., Naidja L. and Bouziane M. (2019). Mass concentrations, seasonal variations, chemical compositions and element sources of PM10 at an urban site in Constantine, northeast Algeria. Journal of Geochemical Exploration. 206, 106356, DOI: 10.1016/j.gexplo.2019.106356.

Bufetova M. (2019). Assessment of income and elimination of heavy metals in the Taganrog bay of the Sea of Azov. Environmental Safety of the Coastal and Shelf Zones of the Sea. 2, 78-85, DOI: 10.22449/2413-5577-2019-2-78-85.

Chance R., Jickells T. and Baker A. (2015). Atmospheric trace metal concentrations, solubility and deposition fluxes in remote marine air over the south-east Atlantic. Marine Chemistry. 177, 45-56, DOI: 10.1016/j.marchem.2015.06.028.

Cheng M.-C. and You C.-F. (2010). Sources of major ions and heavy metals in rainwater associated with typhoon events in southwestern Taiwan. Journal of Geochemical Exploration, 105 (3), 106-116, DOI: 10.1016/j.gexplo.2010.04.010.

Cheng Y., Lee S., Gu Z., Ho K., Zhang Y., Huang Y., Chow J., Watson J., Cao J. and Zhang R. (2015). PM2.5 and PM10-2.5 chemical composition and source apportionment near a Hong Kong roadway. Particuology, 18, 96-104, DOI: 10.1016/j.partic.2013.10.003.

Cheng Y., Liu Y., Huo M., Sun Q., Wang H., Chen Z. and Bai Y. (2011). Chemical characteristics of precipitation at Nanping Mangdang Mountain in Eastern China during spring. Journal of Environmental Sciences. 23(8), 1350-1358, DOI: 10.1016/S1001-0742(10)60560-8.

Cherednichenko V., Cherednichenko A., Cherednichenko Al. and Zheksenbaeva A. (2020). Heavy metal deposition through precipitation in Kazakhstan. Heliyon, 6, e05844, DOI: 10.1016/j.heliyon.2020.e05844.

Chon K., Kim Y., Bae D. and Cho J. (2015). Confirming anthropogenic influences on the major organic and inorganic constituents of rainwater in an urban area. Drinking Water Engineering and Science. 8(2), 35-48, DOI: 10.5194/dwes-8-35-2015.

Christian T., Yokelson R., Cardenas B., Molina L., Engling G. and Hsu S.-C. (2010). Trace gas and particle emissions from domestic and industrial biofuel use and garbage burning in central Mexico. Atmospheric Chemistry and Physics, 10, 565-584, DOI: 10.5194/acp-10-565-2010

Chubarova N., Androsova E., Kirsanov A., Vogel B., Vogel H., Popovicheva O. and Rivin G. (2019). Aerosol and its radiative effects during the Aeroradcity 2018 Moscow experiment. Geography, Environment, Sustainability. 12(4), 114-131, DOI: 10.24057/2071-9388-2019-72.

Chubarova N., Nezval' E., Belikov I., Gorbarenko E., Eremina I., Zhdanova E., Korneva I., Konstantinov P., Lokoshchenko M., Skorokhod A. and Shilovtseva O. (2014). Climatic and environmental characteristics of Moscow megalopolis according to the data of the Moscow State University Meteorological Observatory over 60 years. Russian Meteorology and Hydrology, 39(9), 602-613, DOI: 10.3103/S1068373914090052.

Chubarova N., Zhdanova Ye., Androsova Ye., Kirsanov A., Shatunova M., Khlestova Yu., Volpert Ye., Poliukhov A., Eremina I., Vlasov D., Popovicheva O., Ivanov A., Gorbarenko Ye., Nezval Ye., Blinov D. and Rivin G. (2020). The aerosol urban pollution and its effects on weather, regional climate and geochemical processes. Ed. by N.Ye. Chubarova, Moscow: MAKS Press, DOI: 10.29003/m1475.978-5-317-06464-8

Chudaeva V., Chudaev O. and Yurchenko S. (2008). Chemical composition of precipitation in the southern part of the Russian Far East. Water Resources. 35(1), 58-70, DOI: 10.1134/S0097807808010077.

Cizmecioglu S. and Muezzinoglu A. (2008). Solubility of deposited airborne heavy metals. Atmospheric Research. 89(4), 396-404, DOI: 10.1016/j.atmosres.2008.03.012.

Demetriades A. and Birke M. (2015). Urban geochemical mapping manual: sampling, sample preparation, laboratory analysis, quality control check, statistical processing and map plotting. Brussels: EuroGeoSurveys.

Di Marco V., Tapparo A., Badocco D., D'Aronco S., Pastore P. and Giorio C. (2020). Metal ion release from fine particulate matter sampled in the Po Valley to an aqueous solution mimicking fog water: kinetics and solubility. Aerosol and Air Quality Research. 20(4), 720-729, DOI: 10.4209/aaqr.2019.10.0498.

Elansky N., Ponomarev N. and Verevkin Y. (2018). Air quality and pollutant emissions in the Moscow megacity in 2005–2014. Atmospheric Environment. 175, 54-64, DOI: 10.1016/j.atmosenv.2017.11.057.

Elansky N., Shilkin A., Ponomarev N., Semutnikova E. and Zakharova P. (2020). Weekly patterns and weekend effects of air pollution in the Moscow megacity. Atmospheric Environment. 224, 117303, DOI: 10.1016/j.atmosenv.2020.117303.

Elpat'evskii P. (1993). Geochemistry of migration flows in natural and natural-technogenic geosystems. Moscow, Russia: Nauka.

Eremina I. (2019). Chemical composition of atmospheric precipitation in Moscow and the trends of its long-term changes. Vestnik Moskovskogo Unviersiteta, Seriya Geografiya. 3, 3-10.

Eremina I., Aloyan A., Arutyunyan V., Larin I., Chubarova N. and Yermakov A. (2015). Acidity and mineral composition of precipitation in Moscow: Influence of deicing salts. Izvestiya, Atmospheric and Oceanic Physics, 51(6), 624-632, DOI: 10.1134/S0001433815050047.

Eremina I. and Vasil'chuk J. (2019). Temporal variations in chemical composition of snow cover in Moscow. Geography, Environment, Sustainability, 12(4), 148-158, DOI: 10.24057/2071-9388-2019-79.

Ermolin M., Fedotov P., Ivaneev A., Karandashev V., Fedyunina N. and Burmistrov A. (2018). A contribution of nanoscale particles of road-deposited sediments to the pollution of urban runoff by heavy metals. Chemosphere, 210, 65-75, DOI: 10.1016/j.chemosphere.2018.06.150.

Fabretti J.-F., Sauret N., Gal J.-F., Maria P.-C. and Schärer U. (2009). Elemental characterization and source identification of PM2.5 using Positive Matrix Factorization: The Malraux road tunnel, Nice, France. Atmospheric Research, 94(2), 320-329, DOI: 10.1016/j.atmosres.2009.06.010.

Fedotov P., Ermolin M., Karandashev V. and Ladonin D. (2014). Characterization of size, morphology and elemental composition of nano-, submicron, and micron particles of street dust separated using field-flow fractionation in a rotating coiled column. Talanta, 130, 1-7, DOI: 10.1016/j.talanta.2014.06.040.

Gallorini M. (2000). Trace elements in atmospheric pollution processes: The contribution of Neutron Activation Analysis, In Aerosol Chemical Processes in the Environment, K.R. Spurny, ed, Boca Raton, USA: CRC Press, 431-456.

Galloway J., Thornton J., Norton S., Volchok H. and McLean R. (1982). Trace metals in atmospheric deposition: A review and assessment. Atmospheric Environment, 16(7), 1677–1700, DOI: 10.1016/0004-6981(82)90262-1.

Golubeva N., Matishov G. and Burtseva L. (2005). Precipitation of heavy metals in the Barents Sea region. Doklady Earth Sciences. 401(3), 469-472.

Grigoratos T. and Martini G. (2015). Brake wear particle emissions: a review. Environmental Science and Pollution Research, 22(4), 2491-2504, DOI: 10.1007/s11356-014-3696-8.

Grivas G., Cheristanidis S., Chaloulakou A., Koutrakis P. and Mihalopoulos N. (2018). Elemental composition and source apportionment of fine and coarse particles at traffic and urban background locations in Athens, Greece. Aerosol and Air Quality Research, 18(7), 1642-1659, DOI: 10.4209/aaqr.2017.12.0567.

Kamani H., Hoseini M., Safari G., Jaafari J. and Mahvi A. (2014). Study of trace elements in wet atmospheric precipitation in Tehran, Iran. Environmental Monitoring and Assessment, 186(8), 5059–5067, DOI: 10.1007/s10661-014-3759-9.

Kasimov N., Bezberdaya L., Vlasov D. and Lychagin M. (2019a). Metals, metalloids, and benzo[a]pyrene in PM10 particles of soils and road dust of Alushta city. Eurasian Soil Science, 52(12), 1608-1621, DOI: 10.1134/S1064229319120068.

Kasimov N., Kosheleva N., Vlasov D., Nabelkina K. and Ryzhov A. (2019b). Physicochemical properties of road dust in Moscow. Geography, Environment, Sustainability, 12(4), 96-113, DOI: 10.24057/2071-9388-2019-55.

Kasimov N., Vlasov D. and Kosheleva N. (2020). Enrichment of road dust particles and adjacent environments with metals and metalloids in eastern Moscow, Urban Climate, 32, 100638, DOI: 10.1016/j.uclim.2020.100638.

Konstantinova E., Minkina T., Konstantinov A., Sushkova S., Antonenko E., Kurasova A. and Loiko S. (2020). Pollution status and human health risk assessment of potentially toxic elements and polycyclic aromatic hydrocarbons in urban street dust of Tyumen city, Russia. Environmental Geochemistry and Health, DOI: 10.1007/s10653-020-00692-2.

Kosheleva N., Vlasov D., Korlyakov I. and Kasimov N. (2018). Contamination of urban soils with heavy metals in Moscow as affected by building development. Science of the Total Environment, 636, 854-863, DOI: 10.1016/j.scitotenv.2018.04.308.

Koulousaris M., Aloupi M. and Angelidis M. (2009). Total metal concentrations in atmospheric precipitation from the Northern Aegean Sea. Water, Air, and Soil Pollution, 201(1-4), 389-403, DOI: 10.1007/s11270-008-9952-0.

Kuderina T., Lunin V. and Suslova S. (2018). The geochemical content of precipitation in the forest-steppe landscapes of the Kursk biosphere station. Regional Environmental Issues. 2, 78-83, DOI: 10.24411/1728-323X-2018-12078.

Kumar S., Aggarwal S., Gupta P. and Kawamura K. (2015). Investigation of the tracers for plastic-enriched waste burning aerosols. Atmospheric Environment. 108, 49-58, DOI: 10.1016/j.atmosenv.2015.02.066.

Ladonin D. and Mikhaylova A. (2020). Heavy metals and arsenic in soils and street dust of the Southeastern administrative district of Moscow: long-term data. Eurasian Soil Science, 53(11), 1635-1644, DOI: 10.1134/S1064229320110095.

Ladonin D. and Plyaskina O. (2009). Isotopic composition of lead in soils and street dust in the Southeastern administrative district of Moscow. Eurasian Soil Science, 42(1), 93-104, DOI: 10.1134/S1064229309010128.

Landing W., Caffrey J., Nolek S., Gosnell K. and Parker W. (2010). Atmospheric wet deposition of mercury and other trace elements in Pensacola, Florida. Atmospheric Chemistry and Physics, 10(10), 4867-4877, DOI: 10.5194/acp-10-4867-2010.

Lim B., Jickells T. and Davies T. (1991). Sequential sampling of particles, major ions and total trace metals in wet deposition. Atmospheric Environment, 25(3-4), 745-762, DOI: 10.1016/0960-1686(91)90073-G.

Liu Y., Wang C., Yu Y., Chen Y., Du L., Qu X., Peng W., Zhang M. and Gui C. (2019). Effect of urban stormwater road runoff of different land use types on an urban river in Shenzhen, China. Water, 11(12), 2545, DOI: 10.3390/w11122545.

Liyandeniya A., Deeyamulla M. and Priyantha N. (2020). Source apportionment of rainwater chemical composition in wet precipitation at Kelaniya in Sri Lanka. Air Quality, Atmosphere & Health, DOI: 10.1007/s11869-020-00903-w.

Logiewa A., Miazgowicz A., Krennhuber K. and Lanzerstorfer C. (2020). Variation in the concentration of metals in road dust size fractions between 2 μm and 2 mm: Results from three metallurgical centres in Poland. Archives of Environmental Contamination and Toxicology, 78(1), 46-59, DOI: 10.1007/s00244-019-00686-x.

Long W., Zhou Y. and Liu P. (2020). Numerical simulation of the influence of major meteorological elements on the concentration of air pollutants during rainfall over Sichuan Basin of China. Atmospheric Pollution Research,11(11), 2036-2048, DOI: 10.1016/j.apr.2020.08.019

Loya-González D., López-Serna D., Alfaro-Barbosa J., López-Reyes A., González-Rodríguez H. and Cantú-Silva I. (2020). Chemical composition of bulk precipitation and its toxicity potential index in the metropolitan area of Monterrey, Northeastern Mexico. Environments, 7, 106, DOI: 10.3390/environments7120106.

Ma Y., Tang Y., Xu H., Zhang X., Liu H., Wang S. and Zhang W. (2019). Bulk/wet deposition of trace metals to rural, industrial, and urban areas in the Yangtze River Delta, China. Ecotoxicology and Environmental Safety, 169, 185-191, DOI: 10.1016/j.ecoenv.2018.11.002.

Mamoon A., Jahan S., He X., Joergensen N. and Rahman A. (2019). First flush analysis using a rainfall simulator on a micro catchment in an arid climate. Science of the Total Environment, 693, 133552, DOI: 10.1016/j.scitotenv.2019.07.358.

McHale M., Ludtke A., Wetherbee G., Burns D., Nilles M. and Finkelstein J. (2021). Trends in precipitation chemistry across the U.S. 1985–2017: Quantifyingthe benefits from 30 years of Clean Air Act amendment regulation. Atmospheric Environment. 247, 118219, DOI: 10.1016/j.atmosenv.2021.118219.

Morera-Gómez Y., Alonso-Hernández C., Santamaría J., Elustondo D., Lasheras E. and Widory D. (2020). Levels, spatial distribution, risk assessment, and sources of environmental contamination vectored by road dust in Cienfuegos (Cuba) revealed by chemical and C and N stable isotope compositions. Environmental Science and Pollution Research, 27(2), 2184-2196, DOI: 10.1007/s11356-019-06783-7.

NSAM № 520 AES/MS (2017). Determination of the elemental composition of natural, drinking, sewage and sea waters by atomic emission and mass spectral methods with inductively coupled plasma. Moscow, Russia.

Orlović-Leko P., Vidović K., Ciglenečki I., Omanović D., Sikirić M. and Šimunić I. (2020). Physico-chemical characterization of an urban rainwater (Zagreb, Croatia). Atmosphere, 11(2), 144, DOI: 10.3390/atmos11020144.

Ouyang W., Guo B., Cai G., Li Q., Han S., Liu B. and Liu X. (2015). The washing effect of precipitation on particulate matter and the pollution dynamics of rainwater in downtown Beijing. Science of the Total Environment, 505, 306-314, DOI: 10.1016/j.scitotenv.2014.09.062.

Ouyang W., Xu Y., Cao J., Gao X., Gao B., Hao Z. and Lin C. (2019). Rainwater characteristics and interaction with atmospheric particle matter transportation analyzed by remote sensing around Beijing. Science of the Total Environment, 651, 532-540, DOI: 10.1016/j.scitotenv.2018.09.120.

Özsoy T. and Örnektekin S. (2009). Trace elements in urban and suburban rainfall, Mersin, Northeastern Mediterranean. Atmospheric Research, 94(2), 203-219, DOI: 10.1016/j.atmosres.2009.05.017.

Pan Y. and Wang Y. (2015). Atmospheric wet and dry deposition of trace elements at 10 sites in Northern China. Atmospheric Chemistry and Physics, 15 (2), 951-972, DOI: 10.5194/acp-15-951-2015.

Pan Y.-P., Zhu X.-Y., Tian S.-L., Wang L.-L., Zhang G.-Z., Zhou Y.-B., Xu P., Hu B. and Wang Y.-S. (2017). Wet deposition and scavenging ratio of air pollutants during an extreme rainstorm in the North China Plain. Atmospheric and Oceanic Science Letters, 10(5), 348-353, DOI: 10.1080/16742834.2017.1343084.

Pant P. and Harrison R. (2013). Estimation of the contribution of road traffic emissions to particulate matter concentrations from field measurements: A review. Atmospheric Environment, 77, 78-97, DOI: 10.1016/j.atmosenv.2013.04.028.

Park H., Byun M., Kim T., Kim J.-J., Ryu J.-S., Yang M. and Choi W. (2020). The washing effect of precipitation on PM10 in the atmosphere and rainwater quality based on rainfall intensity. Korean Journal of Remote Sensing, 36(6-3), 1669-1679, DOI: 10.7780/kjrs.2020.36.6.3.4.

Park S.-M., Seo B.-K., Lee G., Kahng S.-H. and Jang Y. (2015). Chemical composition of water soluble inorganic species in precipitation at Shihwa basin, Korea. Atmosphere, 6(6), 732-750, DOI: 10.3390/atmos6060732.

Polyakova O., Artaev V. and Lebedev A. (2018). Priority and emerging pollutants in the Moscow rain. Science of the Total Environment, 645, 1126-1134, DOI: 10.1016/j.scitotenv.2018.07.215.

Popovicheva O., Ivanov A. and Vojtisek M. (2020a). Functional factors of biomass burning contribution to spring aerosol composition in a Megacity: Combined FTIR-PCA analyses. Atmosphere. 11 (4), 319, DOI: 10.3390/atmos11040319.

Popovicheva O., Volpert E., Sitnikov N., Chichaeva M. and Padoan S. (2020b). Black carbon in spring aerosols of Moscow urban background. Geography, Environment, Sustainability. 13 (1), 233–243, DOI: 10.24057/2071-9388-2019-90.

R 2.1.10.1920-04. Human health risk assessment from environmental chemicals (2004). Moscow, Russia: Federal Center for State Sanitary and Epidemiological Supervision of the Ministry of Health of Russia.

Ramírez O., da Boit K., Blanco E. and Silva L. (2020). Hazardous thoracic and ultrafine particles from road dust in a Caribbean industrial city. Urban Climate. 33, 100655, DOI: 10.1016/j.uclim.2020.100655.

Rudnick R. and Gao S. (2014). Composition of the Continental Crust, in Treatise on Geochemistry, Elsevier, 1-51, DOI: 10.1016/B978-0-08-095975-7.00301-6.

Sakata M., Marumoto K., Narukawa M. and Asakura K. (2006). Regional variations in wet and dry deposition fluxes of trace elements in Japan. Atmospheric Environment, 40(3), 521-531, DOI: 10.1016/j.atmosenv.2005.09.066.

Samsonov Y., Ivanov V., McRae D. and Baker S. (2012). Chemical and dispersal characteristics of particulate emissions from forest fires in Siberia. International Journal of Wildland Fire, 21(7), 818, DOI: 10.1071/WF11038.

Schiff K., Tiefenthaler L., Bay S. and Greenstein D. (2016). Effects of rainfall intensity and duration on the first flush from parking lots. Water, 8(8), 320, DOI: 10.3390/w8080320.

Seleznev A., Yarmoshenko I. and Malinovsky G. (2020). Urban geochemical changes and pollution with potentially harmful elements in seven Russian cities. Scientific Reports, 10(1), 1668, DOI: 10.1038/s41598-020-58434-4.

Semenets E., Svistov P. and Talash A. (2017). Chemical composition of atmospheric precipitation in Russian Subarctic. Bulletin of the Tomsk Polytechnic University. Geo Assets Engineering, 328(3), 27-36.

Shen Z., Liu J., Aini G. and Gong Y. (2016). A comparative study of the grain-size distribution of surface dust and stormwater runoff quality on typical urban roads and roofs in Beijing, China. Environmental Science and Pollution Research, 23(3), 2693-2704, DOI: 10.1007/s11356-015-5512-5.

Singh S., Elumalai S. and Pal A. (2016). Rain pH estimation based on the particulate matter pollutants and wet deposition study. Science of the Total Environment. 563–564, 293–301, DOI: 10.1016/j.scitotenv.2016.04.066.

Song F. and Gao Y. (2009). Chemical characteristics of precipitation at metropolitan Newark in the US East Coast. Atmospheric Environment. 43 (32), 4903–4913, DOI: 10.1016/j.atmosenv.2009.07.024.

Song F. and Gao Y. (2011). Size distributions of trace elements associated with ambient particular matter in the affinity of a major highway in the New Jersey–New York metropolitan area. Atmospheric Environment, 45(37), 6714-6723, DOI: 10.1016/j.atmosenv.2011.08.031.

Svistov P., Pershina N., Pavlova M., Polishchuk A. and Semenets E. (2017). Chemical composition of Russian Arctic precipitation in 2007-2015. Russian Meteorology and Hydrology. 2017, 42(5), 314-318, DOI: 10.3103/S1068373917050065.

Talovskaya A., Yazikov E., Filimonenko E., Lata J.-C., Kim J. and Shakhova T. (2018). Characterization of solid airborne particles deposited in snow in the vicinity of urban fossil fuel thermal power plant (Western Siberia). Environmental Technology, 39(18), 2288-2303, DOI: 10.1080/09593330.2017.1354075.

Talovskaya A., Yazikov E., Osipova N., Lyapina E., Litay V., Metreveli G. and Kim J. (2019). Mercury pollution in snow cover around thermal power plants in cities (Omsk, Kemerovo, Tomsk Regions, Russia). Geography, Environment, Sustainability, 12(4), 132-147, DOI: 10.24057/2071-9388-2019-58.

Tian X., Ye A., He Q., Wang Z., Guo L., Chen L., Liu M. and Wang Y. (2020). A three-year investigation of metals in the atmospheric wet deposition of a basin region, north China: Pollution characteristics and source apportionment. Atmospheric Pollution Research, 11(4), 793-802, DOI: 10.1016/j.apr.2020.01.007.

Udachin V., Djedzhi M., Aminov P., Lonshakova G., Filippova K., Deryagin V. and Udachina L. (2010). Chemical composition of atmospheric precipitates of the South Urals. Estestvennie i Tekhnicheskie Nauki, 6, 304-311.

U.S. Borax (2020). Boron in industrial fluids and lubricants. [online] Available at: https://www.borax.com/applications/industrial-fluids-lubricants [Accessed 22 September 2020].

U.S. EPA (2020). RAIS. The Risk Assessment Information System. [online] Available at: https://rais.ornl.gov/ [Accessed 23 September 2020].

Vlasov D., Kasimov N., Eremina I., Shinkareva G. and Chubarova N. (2021a). Partitioning and solubilities of metals and metalloids in spring rains in Moscow megacity. Atmospheric Pollution Research. 2021. Vol. 12. Iss. 1. P. 255-271. DOI: 10.1016/j.apr.2020.09.012

Vlasov D., Kasimov N., and Kosheleva N. (2015). Geochemistry of the road dust in the Eastern district of Moscow. Vestnik Moskovskogo Unviersiteta, Seriya Geografiya, 1, 23-33.

Vlasov D., Kosheleva N. and Kasimov N. (2021b). Spatial distribution and sources of potentially toxic elements in road dust and its PM10 fraction of Moscow megacity. Science of the Total Environment, 761, 143267, DOI: 10.1016/j.scitotenv.2020.143267.

Vlasov D., Vasil'chuk J., Kosheleva N. and Kasimov N. (2020). Dissolved and suspended forms of metals and metalloids in snow cover of megacity: Partitioning and deposition rates in Western Moscow. Atmosphere, 11(9), 907, DOI: 10.3390/atmos11090907.

Vlastos D., Antonopoulou M., Lavranou A., Efthimiou I., Dailianis S., Hela D., Lambropoulou D., Paschalidou A. and Kassomenos P. (2019). Assessment of the toxic potential of rainwater precipitation: First evidence from a case study in three Greek cities. Science of the Total Environment, 648, 1323-1332, DOI: 10.1016/j.scitotenv.2018.08.166.

Weather maps. The World in weather charts (2020). Weather maps. [online] Available at: http://www1.wetter3.de/index_en.html [Accessed 23 September 2020].

Wu Y., Zhang J., Ni Z., Liu S., Jiang Z. and Huang X. (2018). Atmospheric deposition of trace elements to Daya Bay, South China Sea: Fluxes and sources. Marine Pollution Bulletin, 127, 672-683, DOI: 10.1016/j.marpolbul.2017.12.046.

Yanchenko N. and Yaskina O. (2014). Features of chemical composition of snow cover and precipitation in Bratsk. Bulletin of the Tomsk Polytechnic University. Geo Assets Engineering, 324, 27-35.

Yeremina I., Chubarova N., Alexeeva L. and Surkova G. (2014). Acidity and chemical composition of summer precipitation within the Moscow region. Vestnik Moskovskogo Unviersiteta, Seriya Geografiya, 5(5), 3-11.

Yu J., Yan C., Liu Y., Li X., Zhou T. and Zheng M. (2018). Potassium: a tracer for biomass burning in Beijing? Aerosol and Air Quality Research, 18(9), 2447-2459, DOI: 10.4209/aaqr.2017.11.0536.

Zheng J., Zhan C., Yao R., Zhang J., Liu H., Liu T., Xiao W., Liu X. and Cao J. (2018). Levels, sources, markers and health risks of heavy metals in PM2.5 over a typical mining and metallurgical city of Central China. Aerosol Science and Engineering, 2(1), 1-10, DOI: 10.1007/s41810-017-0018-9.